JOURNAL OF MATERIALS SCIENCE 14 (1979) 2906–2912

On the decomposition behaviour of Al–4.5 at% Zn–2 to 3 at% Mg alloys during continuous heating

M. RADOMSKY, O. KABISCH, H. LÖFFLER
Pädagogische Hoschschule Halle, Sektion Mathematik/Physik, Halle/Saale, GDR
J. LENDVAI, T. UNGÁR, I. KOVÁCS, G. HONYEK
Institute for General Physics, Loránd Eötvös University, Budapest, Hungary

The decomposition processes taking place in the Al–4.5 at % Zn–2 to 3 at % Mg alloys were studied during continuous heating by means of electrical resistivity, XSAS and DSC measurements and by TEM investigations. It was found that the room temperature pre-ageing has no significant influence on the processes taking place above 230° C. Several temperature ranges were determined in which the decomposition of the solid solution and/or the transformation of the different particles of the second phases take place by different mechanisms.

1. Introduction

A large number of papers have been concerned with the zone formation and the precipitation processes in the Al–Zn–Mg ternary alloy system [1–4]. It was found that in the Al-rich ternary alloys the decomposition takes place by the formation of GP zones up to about 100° C. At higher temperatures several precipitation processes were determined. In the case of not very low Zn:Mg ratios the $MgZn_2$ type η' transition phase and the stable η phase were observed [2, 4, 5]. With higher Mg content the stable $Mg_3Zn_3Al_2$ type ternary phase is also present at higher temperatures [2, 4]. Since the formation of the more stable phases in the alloy system is preceded in many cases by the formation of GP zones and/or fully or partially coherent precipitates, several solid state reactions can take place at different temperatures between the different second phases [4, 6].

The aim of the present work was to study the precipitation processes in the Al–4.5 at % Zn–x Mg alloys over a wide range of temperature, and to clarify how the different metastable phases dissolve or transform to more stable ones at different temperatures. The measurement of various parameters (X-ray small angle scattering, electrical resistance, calorimetry and TEM) during continuous heating proved to be a powerful method in localizing the main processes in the different temperature ranges, although it has to be taken into account that due to the continuously varying temperature the alloy is not in the state of metastable equilibrium during most of the investigations.

2. Experimental procedure

The Al–4.5 at % Zn–x Mg alloys investigated were prepared from 4 N material with $x = 2$ and 3 at %. The samples were solution heat-treated for ½ h at 490° C, quenched in r.t. water and then heated with a constant heating rate after different periods of pre-ageing at r.t.

The integral intensity (II) of XSAS was measured *in situ* by a Kiessing-type XSAS camera, the intensity distribution curves (IDC) of XSAS were determined by a Kratky-type XSAS camera. The electrical resistance of the samples was measured by a method in which a constant current was applied and the voltage drop on the sample minus a temperature dependent counter-voltage (compensating for the temperature dependent part of the resistance) was recorded as a function of

0022–2461/79/122906–07$02.70/0

temperature on an X–Y recorder. The method has been described in more detail elsewhere [7].

Calorimetric measurements were performed by a Perkin–Elmer DSC-2 differential scanning calorimeter. The TEM investigations were made on a Tesla BS 540 electron microscope operating at 120 kV.

The XSAS II and the reduced electrical resistance were measured at a heating rate of $10\,K\,min^{-1}$. The IDC were taken after heating the specimens at the same heating rate to a temperature, T_i and then quenching them to r.t. The TEM investigations were made in the same way, but the heating rate in this case was $20\,K\,min^{-1}$, while the heating rate in the DSC measurements was $80\,K\,min^{-1}$. Because of the relatively high heating rate the characteristic temperatures determined from the calorimetric measurements may be shifted to somewhat higher temperatures than those obtained from the other measurements.

3. Experimental results

The influence of the r.t. pre-ageing on the processes taking place during continuous heating is clearly shown in Fig. 1, where the changes in the reduced resistance, ΔR are shown for the alloy Al–4.5 at % Zn–3 at % Mg as a function of temperature after different periods of r.t. pre-ageing ranging from 0 to 120 days. The behaviour of the alloy with 2 at % Mg was found to be essentially the same.

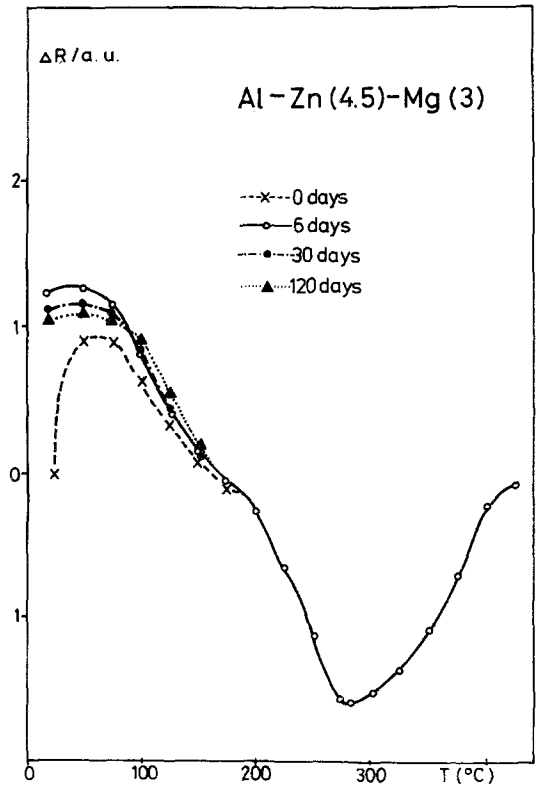

Figure 1 The changes in electrical resistivity during continuous heating at a rate of $10\,K\,min^{-1}$ after different pre-ageing at r.t. Samples were solution heat treated before r.t. ageing at 480° C for 30 min.

The ΔR–T curve measured immediately after quenching shows the well-known maximum of the electrical resistivity caused by the formation of small (subcritical) GP zones [7]. The initial increase of ΔR becomes smaller with increasing the time of r.t. ageing. This can be easily understood taking into account that during the r.t. ageing the zone-size exceeds the critical value. On the other hand a slight increase in ΔR can be observed even after longer periods of pre-ageing, which indicates that the decomposition of the supersaturated solid solution is not complete even after 120 days of r.t. ageing and during the subsequent heating the amount of subcritical GP zones increases up to about 60° C.

The ΔR–T curves become independent of the pre-ageing time above about 190° C indicating that the further reactions occurring upon heating are – to a good approximation – independent of the period of pre-ageing.

Samples aged at r.t. for 50 days were heated at $80\,K\,min^{-1}$ in a DSC-2 calorimeter. As soon as 420° C was attained the samples were cooled down to −60° C at a rate of $320\,K\,min^{-1}$. After this an immediate second heating was performed (Fig. 2). According to our control measurements the above-mentioned cooling rate is sufficient to preserve the solid solution state during the cooling process.

The second heating can be regarded as starting from the solid solution state, to a good approximation. In this sense the second heating curves can be regarded as corresponding to the heating of quenched specimens. It should be mentioned, however, that the vacancy concentration in this case might be lower than in quenched specimens. On the thermograms starting from the solid solution state (second heating) an exothermic reaction can be observed from about 30 up to about 140° C, which corresponds to the formation and growth of GP zones. This exothermic reaction is followed by an endothermic one between about 140 and 180° C, indicating that in this temperature range the main process is the dissolution of the

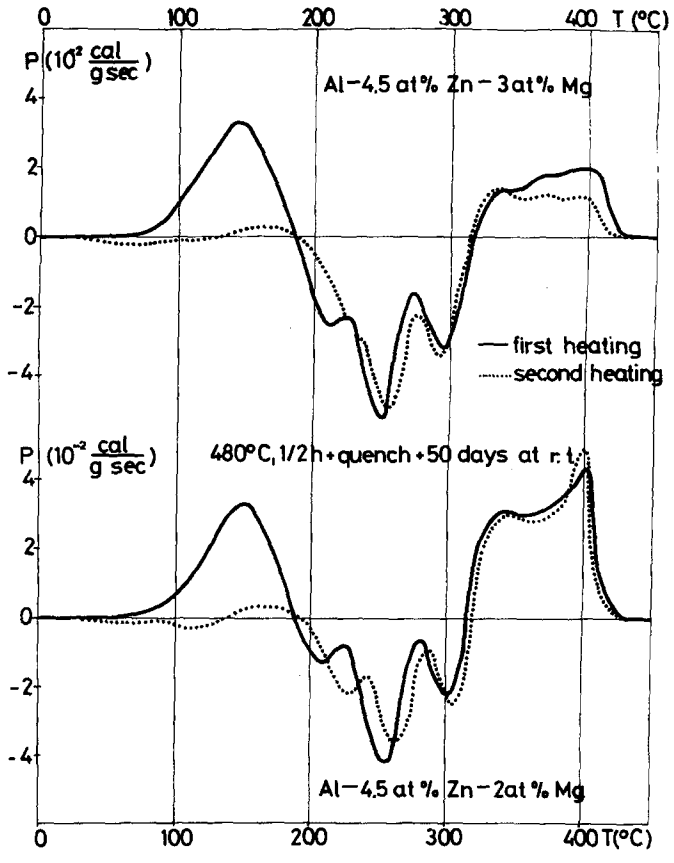

Figure 2 DSC-2 thermograms of samples pre-aged for 50 days at r.t. (continuous line) and after rapid cooling from 420° C (dashed line).

pre-existing particles. The thermograms measured after 50 days pre-ageing at r.t. start with a large endothermic peak which obviously corresponds to the dissolution of the GP zones formed during the r.t. pre-ageing.

The transition from endothermic to exothermic reaction takes place at about 190° C in the case of all four thermograms, i.e. at the same temperature where the $\Delta R-T$ curves become independent of the pre-ageing time. According to the DSC curves there are certain differences between the first and second heating at least up to about 230° C, indicating that the precipitation process does depend slightly on the r.t. pre-ageing even in this temperature range. The three peaks in the thermograms between 190 and 310° C show clearly that the precipitation in this temperature range takes place in three stages.

According to our earlier investigations [8, 9] and to the XSAS II measurements shown in Fig.

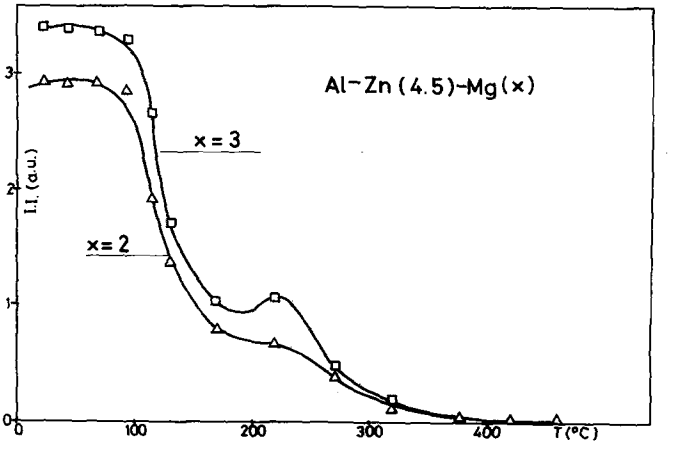

Figure 3 The changes of the integral intensity of XSAS during continuous heating. The *in situ* measured intensity scattered in the angle range between 0.4 and 3.5 degrees in 2θ was divided by the Guinier radii corresponding to different temperatures in Fig. 4. Samples were solution heat treated and pre-aged at r.t. for 3 months before heating.

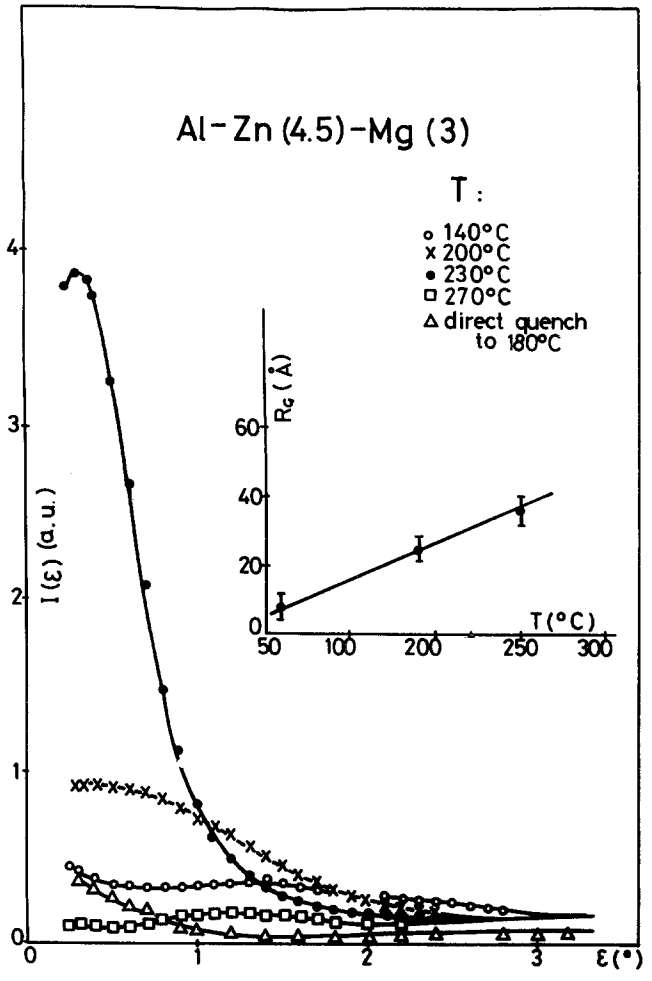

Figure 4 XSAS intensity distribution curves and Guinier radii of samples quenched to r.t. and heated immediately to temperatures, T_i by 10 K min^{-1}

3, the reversion of GP zones in the alloys investigated is only partial; i.e. not all the GP zones dissolve before the formation of the metastable η' phase starts. This is clearly demonstrated by the changes in II (Fig. 3), namely the minimum value of the II is much higher than that corresponding to the solid solution state. After attaining the minimum at about 160° C the II is increasing again, due to the formation of the metastable η' particles.

XSAS experiments were carried out on samples solution heat treated and then heated up to different temperatures, T_i, at a rate of 10 K min^{-1}. The intensity distribution curves were taken at r.t. and are shown in Fig. 4. It can be seen that the scattered intensity is increasing monotonically when T_i is raised up to about 230° C. At $T_i = 275°$ C, however, practically no XSAS can be observed. The small scattering in the angle range between 1 and 2 degrees is most probably due to some very small zones formed during cooling the sample and/or during the measurement at r.t. The lack of XSAS in this state of the alloy indicates that there are no particles in the alloy with an average size smaller than about 10 nm. The same figure shows that the Guinier radius of the precipitates increases with increasing value of T_i. A careful inspection of the intensity distribution curves indicates that up to about 200° C the particles have a large dispersity whereas if T_i is higher than 200° C larger particles with smaller dispersity are present in the alloy. This fact is further supported by the following TEM investigations.

The TEM picture taken after heating with 20 K min^{-1} from r.t. to 200° C (Fig. 5a) shows small spherical precipitates with a radius of about 2.5 nm. The corresponding selected area diffraction pattern in Fig. 5c shows definite reflections which do not belong to the matrix. At the same time the strict regularity of the extra diffraction spots indicates that the precipitates have a strong

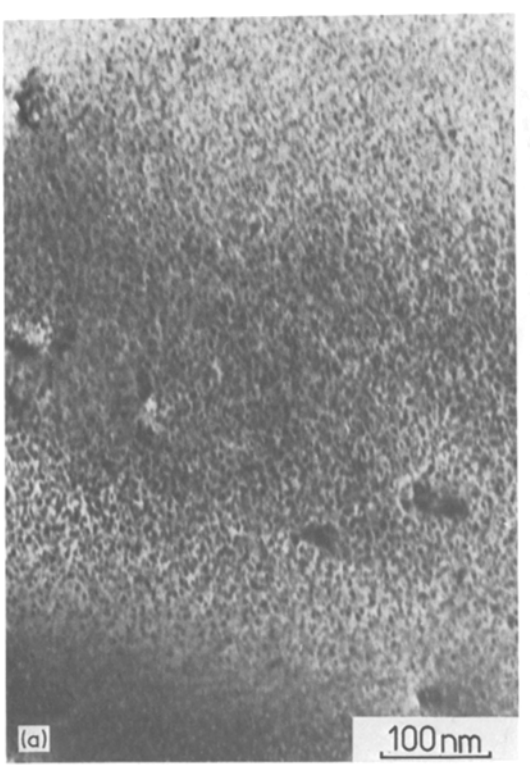

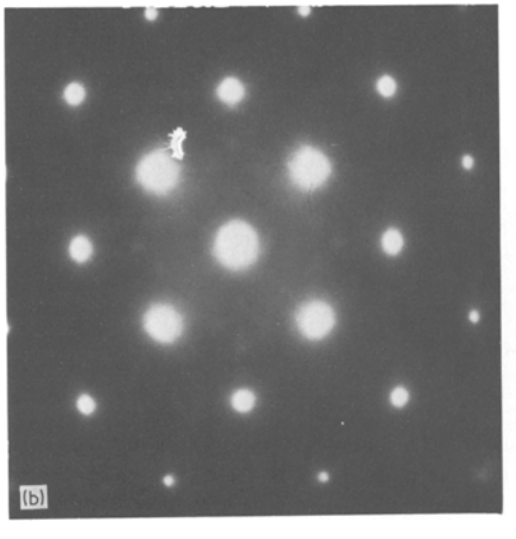

Figure 5 TEM picture and diffraction pattern of an Al–4.5 at% Zn–3 at% Mg sample quenched to r.t. and heated immediately to 200° C at 20 K min^{-1}.

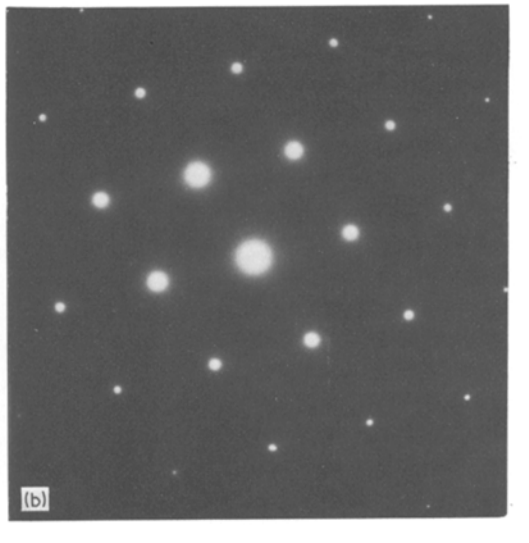

Figure 6 TEM picture and diffraction pattern of an Al–4.5 at% Zn–3 at% Mg sample quenched to r.t. and heated immediately to 230° C at 20 K min^{-1}.

correlation with the matrix orientations. On the basis of this, these particles are coherent pre-precipitates of the η' phase.

The micrograph and the corresponding diffraction pattern of samples heated up to 230° C at 20 K min^{-1} are shown in Fig. 6. Fig. 6a shows small particles of the η' phase. In Fig. 6b. very vague streaks in the $\{1\,1\,1\}^*_\alpha$ direction can be observed indicating the existence of a strain field slightly modifying the mean spacing of the $\{1\,1\,1\}_\alpha$ planes. This fact shows that these particles are coherent with the matrix along the $\{1\,1\,1\}_\alpha$ plane.

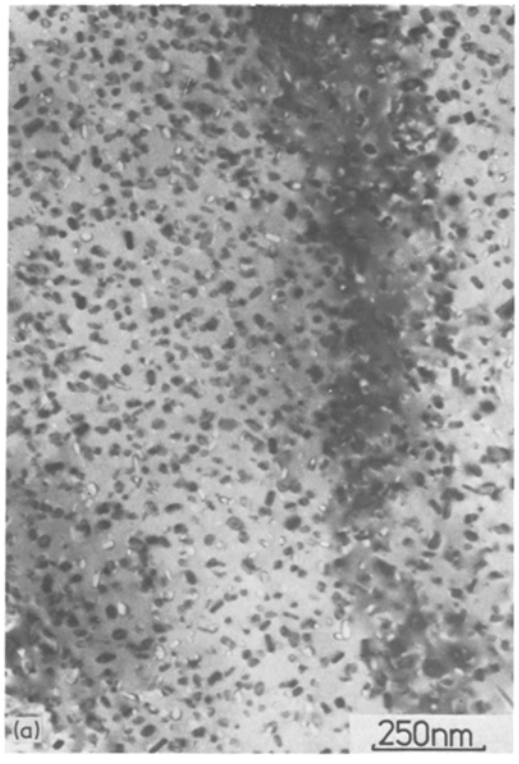

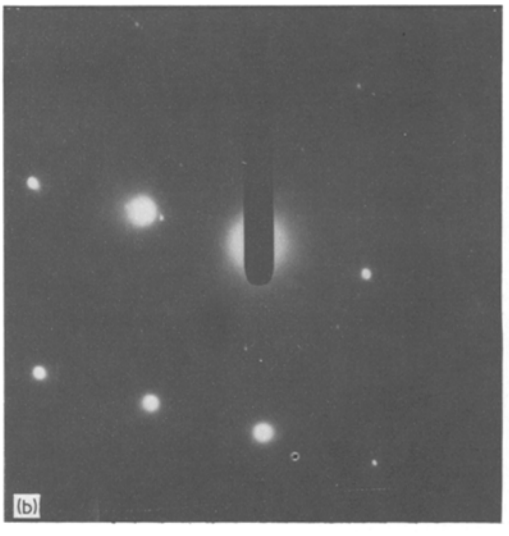

Figure 7 TEM picture and diffraction pattern of an Al–4.5 at% Zn–3 at% Mg sample quenched to r.t. and heated immediately to 275° C at 20 K min^{-1}.

Fig. 7 shows the micrograph and diffraction pattern of samples heated to 275° C at 20 K min^{-1}. Rod-shaped particles of mean size about 10 nm can be seen in Fig. 7a. The irregular localization of the extra diffraciton spots along a Debye–Scherrer ring in Fig. 7b indicates that the precipitates have random orientations relative to the matrix, characteristic of the incoherent particles of the η phase [4, 5].

4. Discussion

On the basis of these results several temperature ranges can be determined in which the decomposition of the solid solution state and/or the transformation of the different particles of the second phases take place by different mechanisms.

The first temperature range can be placed between r.t. and about 70° C. The decomposition of the solid solution state takes place by the formation and growth of subcritical GP zones. The Guinier radius, R_G, does not exceed 1 nm even at 70° C (Fig. 4). At the same time there is practically no change in the zone state of the alloy after long term r.t. ageing during heating up to about 70° C. This is indicated by the constancy of II (Fig. 3), P (Fig. 4) and ΔR (Fig. 1) up to this temperature.

In the temperature range between 70 and about 130° C the dissolution and/or Ostwald ripening of GP zones takes place. This is indicated by the strong decrease in ΔR and the increase of R_G in Figs. 1 and 4. The exothermic reaction during the second heating in Fig. 2 shows that the energy released by the growth of the large GP zones overcompensates the heat of dissolution of the smaller ones. At the same time it can be seen from Figs. 2 and 3 that a considerable dissolution of GP zones formed during long term ageing at r.t. takes place in this temperature range.

In the temperature range between 130 and about 200° C the basic process is the dissolution of GP zones formed at lower temperatures which is indicated by the second heating curve in Fig. 2. The rate of change of ΔR decreases in this temperature range indicating that the growth of larger zones is slowed down.

In samples pre-aged at r.t. for a long period of time the dissolution of GP zones can be observed in Fig. 1 to 3. From above 150° C, however, the nucleation of the η' particles begins and at higher temperatures these two processes are overlapping (Fig. 2).

Between 200 to 300° C the II is strongly decreasing (Fig. 3) caused by the shifting of the XSAS intensity to very small angles which are excluded from observation in the present apparatus. ΔR is also strongly decreasing in this temperature range (Fig. 1) and attains its minimum value at

about 280° C indicating that the amount of precipitated material is the highest at this temperature. This is in agreement with the results of the calorimetric measurements (Fig. 2) from which it can be seen that the exotherm reactions end at about 300° C. It is clearly shown by the thermograms that the precipitation process between 200 and 300° C takes place in three steps. Up to about 230° C the nucleation and growth of the η' phase takes place (Figs. 5 and 6). In the range between 230 and about 270° C the $MgZn_2$ type η phase is precipitating (Fig. 7). Above about 270° C the third exotherm reaction in Fig. 2 indicates the formation of a third type of precipitate. On the basis of the ternary phase diagram of Al–Zn–Mg [4] this phase is most probably of $Mg_3Zn_3Al_2$ type.

Above 300° C the dissolution of the precipitated second phases starts, as indicated by the increase of ΔR in Fig. 1 and the endotherm reactions in Fig. 2. According to both types of measurements the solid solution state is attained above about 420° C in good agreement with the phase diagram of the alloy [4].

5. Conclusions

Applying different techniques to follow the precipitation sequence in the Al–4.5 at % Zn–2 to 3 at % Mg alloy system it was possible to determine the precipitate phases forming in different temperature ranges. The observed basic processes are summarized as follows:

Temperature range	Processes
20 to 70° C	Formation and growth of GP zones
70 to 130° C	Coarsening of GP zones
130 to 200° C	Dissolution of GP zones; nucleation of η' precipitates
200 to 230° C	Further nucleation and growth of η' particles
230 to 270° C	Formation of the $MgZn_2$ type η' phase
270 to 300° C	Formation of the $Mg_3Zn_3Al_2$ type phase
300 to 420° C	Dissolution of the precipitates.

References

1. R. GRAF, *Compt. Rend.* **242,** (1956) 1311.
2. H. SCHMALZRIED and V. GEROLD, *Z. Metallkde.* **49** (1958) 291.
3. O. KAWANO, Y. MURAKAMI, T. NAKAZAWA and K. S. LIU. *Trans. Japan Inst. Metals* **11** (1970) 12.
4. L. F. MONDOLFO, *Met. Rev.* **153** (1971) 95.
5. P. A. THACKERY, *J. Inst. Metals* **96** (1968) 228.
6. N. RYUM, *Z. Metallkde.* **66** (1975) 338.
7. K. H. SACKEWITZ, H. LÖFFLER and R. KROGGEL, *Neue Hütte* **21** (1976) 241.
8. G. GROMA, E. KOVÁCS-CSETÉNYI, I. KOVÁCS, J. LENDVAI and T. UNGÁR, *Z. Metallkde.* **67** (1976) 404.
9. T. UNGÁR, J. LENDVAI, I. KOVÁCS, G. GROMA and E. KOVÁCS-CSETÉNYI, *ibid* **67** (1976) 683.

Received 30 March and accepted 11 May 1979.